321 Tb/s E/S/C/L-band Transmission with E-band Bismuth-Doped Fiber Amplifier and Optical Processor

Benjamin J. Puttnam, *Member, IEEE,* Ruben S. Luís, *Senior Member, IEEE,* Yetian Huang, *Member, IEEE,* Ian Phillips, *Member, IEEE,* Dicky Chung, *Member, IEEE,* Nicolas K. Fontaine, *Member, IEEE,* Budsara Boriboon, G. Rademacher, Senior Member, IEEE, Mikael Mazur, Member, IEEE, Lauren Dallachiesa, Member, IEEE, Haoshuo Chen, *Member, IEEE,* Wladek Forysiak, *Member, IEEE,* Ray Man, *Senior Member, IEEE,* Roland Ryf, *Senior Member, IEEE,* David T. Neilson, *Fellow, IEEE,* and Hideaki Furukawa, *Member, IEEE.*

***Abstract*—Using a newly developed E-band bismuth doped fiber amplifier and multi-port optical processor, we investigate wideband E/S/C/L-band transmission with signal bandwidths up to 27.8 THz and distances up to 200 km. Dense wavelength-division multiplexed (D-WDM) transmission is enabled by using a combination of thulium and erbium and bismuth doped-fiber amplifiers in combination with distributed Raman amplification. For 50 km transmission, we transmit a wideband DWDM signal comprising 1097 channels covering 212.3 nm (27.8 THz) from 1410.8 nm to 1623.1 nm for a record single-mode fiber (SMF) data-rate of 321 Tb/s (301 Tb/s after decoding), an increase of 25% on the previous record data-rate. We further show single span transmission at 100 km and 150 km before recording 270.9 Tb/s (258.1 Tb/s after decoding) for 200 km transmission over 2 amplified spans. These results show the potential of E-band transmission, to increase the information carrying capability of optical fibers and open the door to multi-band fiber networks built on already deployed fibers.**

***Index Terms*—Wideband transmission, Multi-band transmission, Raman amplifier, Optical amplifier**

I. INTRODUCTION

Demand for enhanced data transmission capacity [1-2] has inspired investigation of both additional spectral windows [3-4] and new fibers utilizing the spatial domain [5-6]. Of these approaches, adopting new transmission windows offers a potentially significant benefit in the near-term as a method of extending the useful lifespan of deployed optical fibers [4] to provide additional transmission capacity without large capital expenditure associated with new fiber deployment. Combining multi-band systems with high-order modulation and dense wavelength division multiplexing (DWDM) is a promising approach to fully exploit deployed fiber capacity. The maturing of hollow core fiber technology also offers the prospect of a low-loss broadband fiber transmission window that further encourages development of wideband transmission eco-system [7].

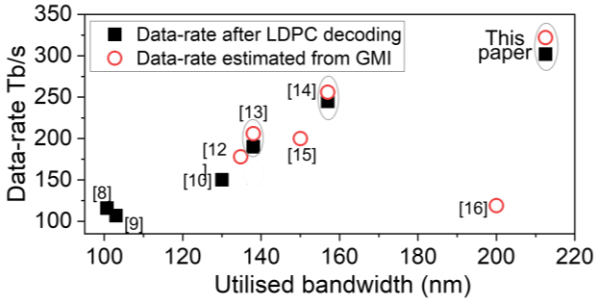

Fig. 1: Wideband (> 100nm) transmission demonstration exceeding 100 Tb/s in SMF [7-16]

However, moving away from the low-loss window of standard single-mode fibers (SMFs) necessitates new amplification schemes beyond the standard erbium-doped fiber amplifier (EDFA) that is a staple of C-band or C + L-band systems. Previously, S/C/L-band transmission has been explored with various amplifier technologies. Semiconductor optical amplifiers (SOAs) have been used to demonstrate 100 km transmission with >100 nm amplification in a single device covering S to L-bands [8] and their combination with distributed Raman amplification enabled transmission over 300 km of SMF [9]. To increase transmission bandwidths, C/L-band EDFAs, have been combined with complimentary amplification schemes including distributed Raman amplification [10], thulium doped-fiber amplifiers (TDFAs) [11] and combined TDFA/discrete Raman amplification [12]. Various demonstrations have combined TDFA, EDFA and distributed Raman amplification [13] culminating in 244 Tb/s decoded throughput utilizing 157 nm bandwidth [14] and 200.5 Tb/s transmission over 200 km [15]. More recently, wideband transmission has expanded further with O-band combined with S/C/L and U-band transmission for 119 Tb/s transmission with a 25 THz signal bandwidth in a deployed fiber [16].

Ben Puttnam, Ruben Luis, Budsara Boriboon, and Hideaki Furukawa are members of the Network System Institute at The National Institute of Information and Communications Technology, 4-2-1 Nukui-Kitamachi, Koganei, Tokyo 184-8795, Japan. (e-mail: ben@nict.go.jp).

Yetian Huang, Nicolas K. Fontaine, Mikael Mazur, Lauren Dallachiesa, Haoshuo Chen, Roland Ryf, and David T. Neilson are with Nokia Bell Labs, 600 Mountain Ave, New Providence, NJ 07974, USA

Wladek Forysiak and Ian Phillips are with Aston Institute of Photonic Technologies, Aston University, Birmingham, UK,

Dicky Chung and Ray Man are with Amonics PLC,14F Lee King Industrial Building, Kowloon, Hong Kong.

Georg Rademacher is with the University of Stuttgart, 70174 Stuttgart, Germany.

Here, we expand on the results presented in [17], [18], investigating DWDM transmission with DFAs and distributed Raman amplification for E/S/C/L-band transmission over distances up to 200 km. For single span transmission at 50 km we transmit a wideband DWDM signal comprising 1097 channels covering 212.3 nm (27.8 THz) from 1410.8 nm to 1623.1 nm, over the E, S, C and L-bands. E-band transmission was achieved using distributed Raman amplification, a newly developed bismuth-doped fiber amplifier (BDFA) and a multi-port E-band optical processor (OP) for gain equalization. For comparison purposes, Fig. 1 shows >100 Tb/s transmission demonstrations with bandwidths exceeding 100 nm. Our achieved GMI estimated data-rate of 321 Tb/s after 50 km transmission exceeds the previous highest single-mode fiber (SMF) data-rate [14] by over 25% and the near continuous transmission bandwidth of 212.3 nm is also a 35% increase.

Next, we investigate single span transmission up to 150 km before selecting 100 km spans to investigate amplified two-span transmission over 200 km for 1050 x 24.5 GBd PDM 64-QAM channels from 1416.3 nm to 1622.7 nm. Compared to the results presented in [18], we improve the overall data-rate by optimization of the modulator stability, increasing the data-rate to 270.9 Tb/s and decoded throughput to 258.1 Tb/s. These results show wideband transmission over more than 200 nm signal bandwidth can not only significantly improve SMF data-rates but has potential for transmission of such bandwidths over multi-span amplified links. Collectively these results show that E/S/C/L-band transmission enabled by a new BDFA and multi-port OP can increase the information carrying capability of new and deployed optical fibers.

II. Description of BDFA and Multi-Port Optical Processor

E-band amplification was achieved by newly developed germanium-co-doped BDFAs. A number of BDFA [19], [20], [21] and Raman supported [22] demonstrations have shown gain over bandwidths as high as 195 nm and 210nm, respectively, covering the E-band and neighbouring S-band wavelength ranges. 115 nm and more gain bandwidths have also been achieved across the O and E-bands by adopting BDFAs [23], [24]. However, to reach our target of supporting DWDM transmission of high-order QAM signals over multiple amplification stages, the BDFA design here focussed on high gain and output power over a reduced bandwidth of around 55 nm (6 THz) in the E-band. The amplified spontaneous emission (ASE) spectrum of the manufactured BDFA is shown in Fig. 2(a). The amplifier contained about 150 m of active fiber that was pumped with 700 mW laser diodes at 1310 nm for a maximum output power of 24 dBm. The noise figure of 5 wavelength channels across the band were measured to be between 5.7 dB to 4.7 dB for 0 dBm input power, as shown in Fig. 2 (b). The gain of the same channels varied from 22 dB and 25.5 dB, as shown in Fig. 2(c).

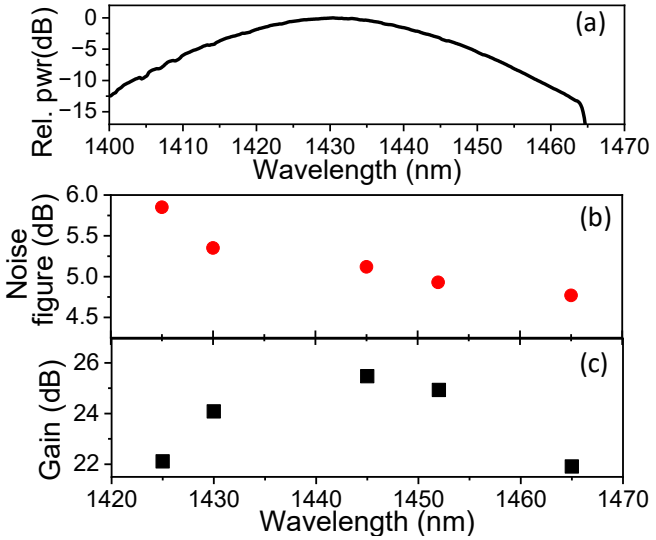

Fig. 2: (a) ASE spectrum without signal input, (b) noise figure and (c) gain for 5 wavelengths with 0 dBm input power

Another key component of the new E-band transmission system was the optical processor (OP) or dynamic gain equalizer/blocker. As with S/C/L-bands as described in the next section, OPs were used use shape the transmission spectrum and make a notch in the transmitted spectrum to accommodate the test-channels. The OP was particularly crucial in E-band since the BDFAs did not contain a gain-flattening filter (GFF) used in the thulium and erbium DFAs. The custom developed multi-port E-band OP [25] was an LCOS based device and contained 18 individual 1 x 1 ports operating from 1400 nm to 1465 nm.

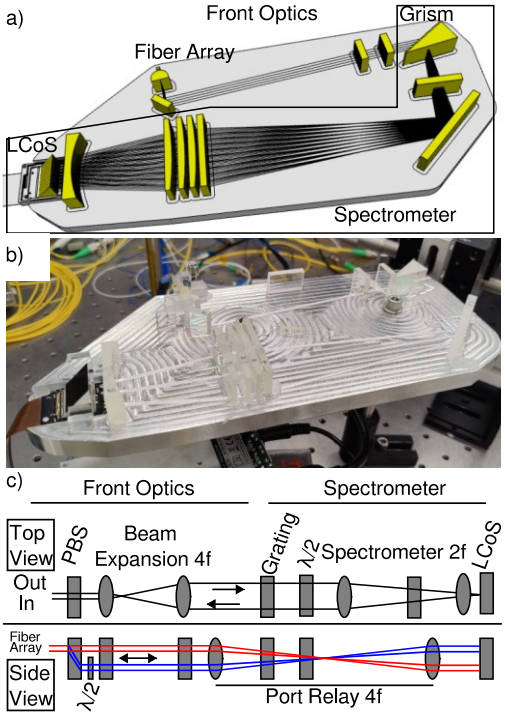

Fig. 3: E-Band optical processor (a) ray simulation and mechanical model of wavelength equalizer with cylindrical optics and dispersion grating mounted on prism to linearize spectrum, (b) image of packaged blocker assembled on base plate, and, (c) Schematic for wavelengths (top view) and ports (side view)

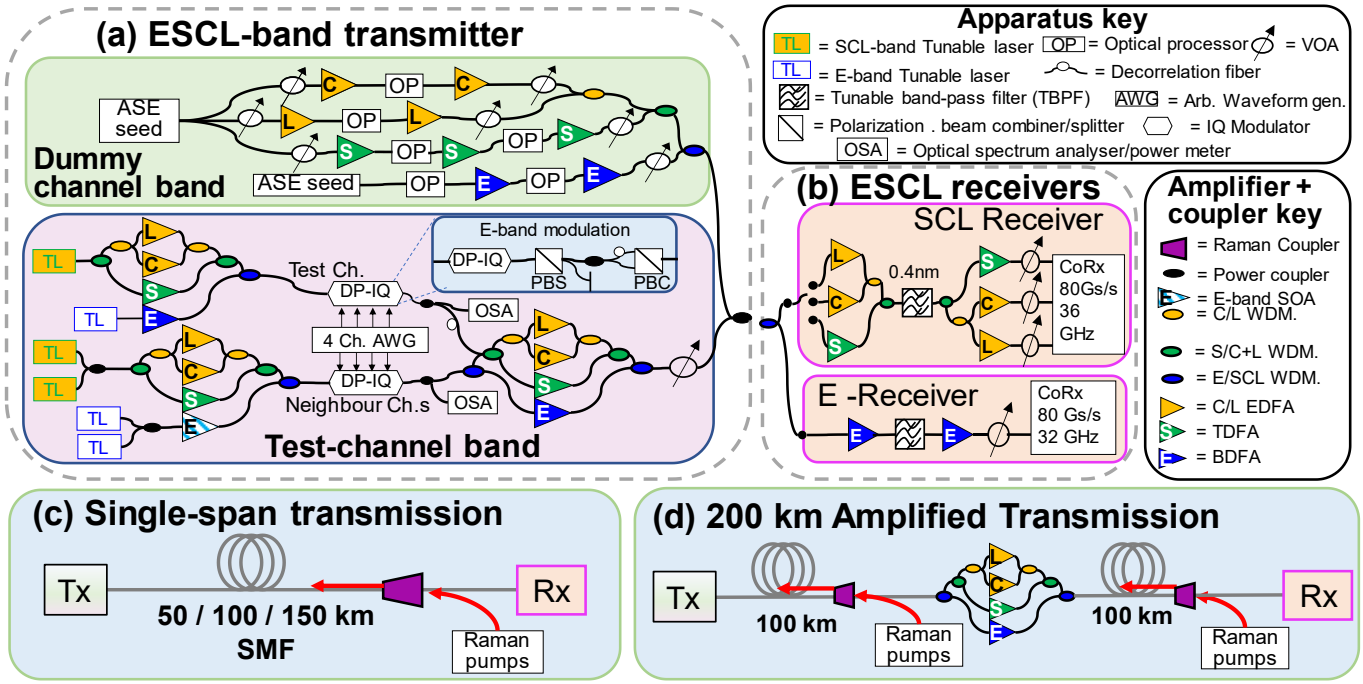

Fig. 4: Transmission set-up showing (a) ESCL-band transmitter (b) SCL and E-band receiver set-up, (c) transmission scheme for single-span transmission over 50 km, 100 km and 150 km and (d) transmission for 200 km amplified transmission.

The E-band OP shown in Fig. 3 uses transmission grating with a 1.2 µm period originally intended for the O-Band, with the incidence angle rotated to 59 degrees to optimize performance in the E-Band. The gating is mounted on a low index glass prism that partially linearizes the spectral dispersion. The optical system consists of front optics that expand the beams and provide required polarization diversity for the grating and LCoS and spectrometer optics that image the dispersed wavelengths onto the LCoS.

The minimum loss measured for a single pass was 5 dB but the insertion loss of all ports was observed to increase to around 9 dB after shipping. For all transmission experiments the OP was able to flatten the BDFA spectrum and generate a deeper than 40 dB notch with a double pass of the LCOS and amplification between passes. The roll-off of the passband edges was approximately 1 GHz/dB with some variation between wavelength channels.

III. Experiment Description

The same transmitter and receiver set-ups, shown in Fig. 4(a, b), were used for all transmission experiments with 2 distinct transmission set-ups used for single span transmission up to 150 km and 200 km two-span transmission. The transmitter set-up comprised a sliding 3 channel test-band within a wideband WDM signal constructed from spectrally shaped ASE noise, as shown in Fig. 4(a). The test-band consisted of a test-channel and 2 neighbouring channels originating from 10 kHz linewidth tunable lasers for S/C/L-band channels and 200 kHz linewidth TLs for E-band signals. Amplification was achieved in 4 DFA variants. EDFAs were used for C and L-band signals whilst S-band signals were amplified in TDFAs and the BDFAs described in the previous section was used for amplifying E-band signals. In addition to the BDFA, an E-band SOA was used to amplify the neighbour channels of the test-band. The TDFAs had around 20 dBm output power and noise figure <7 dB and the EDFAs had various output powers and noise figures of <5 dB and < 6 dB for C-band and L-band respectively. The test and neighbour channels were modulated in dual-polarization IQ-modulators (DP-IQ) driven by the data and data-bar outputs of four arbitrary waveform generators (AWGs) operating at 49 GS/s with optical patch cords used for signal decorrelation. These produced 24.5 GBd, PDM-16, 64 or 256 QAM root-raised cosine shaped signals with a roll-off of 0.01 based on 2^{16}-1 bit pseudo-random binary sequences. 20 dB taps were used to monitor the modulated signals.

The same modulator was used for E-band modulation. However, it was observed that wavelength dependence of a polarization beam splitter (PBS) in the modulator severely degraded modulation quality in one polarization. Hence, E-band signals were split in a wideband PBS after the modulator with the high-quality single polarization signal sent to a PDM emulator, with a 3 m polarization maintaining patch cord used for signal decorrelation, as shown in the inset of the test-band panel of Fig. 4 (a).

Dummy wavelength channels were generated from ASE noise shaped using band-specific OPs, as in [26], and further amplified in the appropriate B/T/E-DFA. The Launch power was set to around -4 dBm per channel for a total launch power of around 26 dBm. The OPs were used to carve a sliding 80 GHz wide notch in the dummy channel spectrum to accommodate the current test-channel. The S/C/L-band OPs were commercial devices with the OP described in the previous section used for E-band.

In each band, the receiver paths, shown in Fig, 4(b) consisted

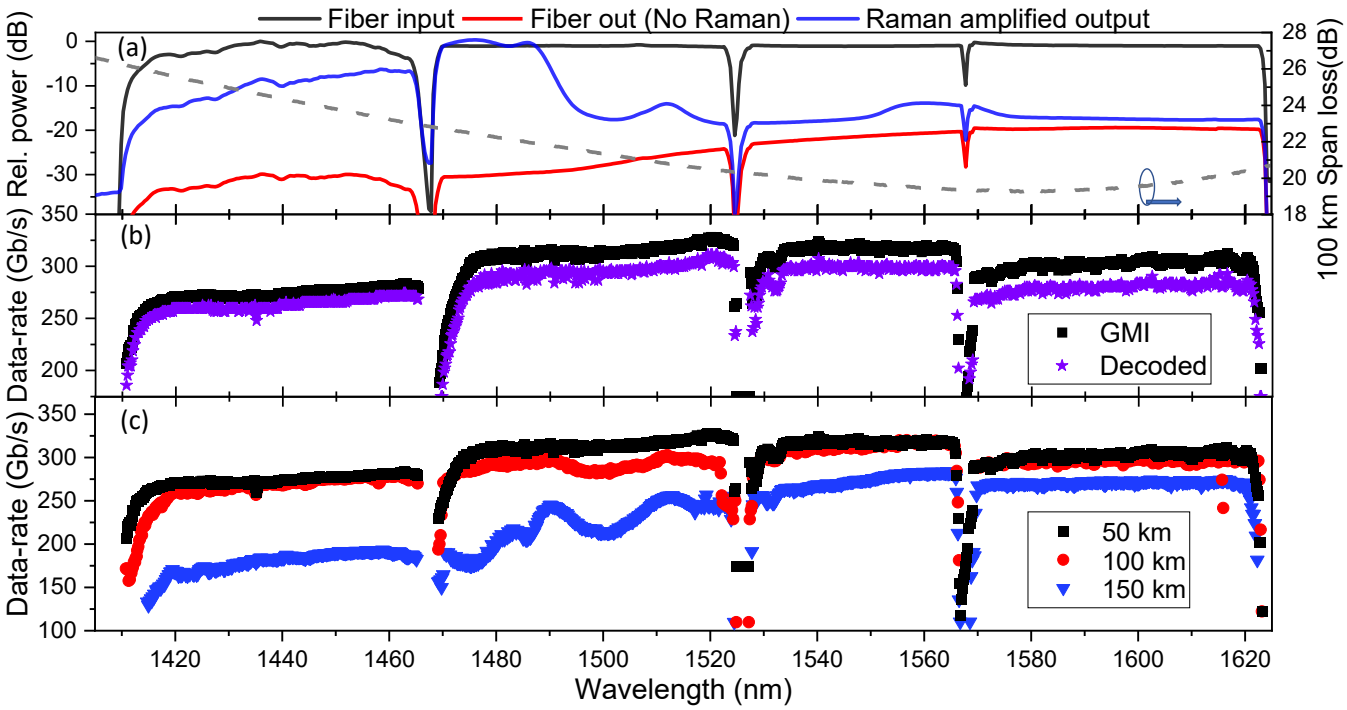

Fig. 5: Left-axis – E/S/C/L-band signal at input (black) + output (red) of first fiber span with Raman amplification profile (blue). Right-axis span loss of 100 km fiber (b) GMI estimated and LDPC decoded data-rate after 50 km transmission, and (c) GMI estimated data-rate after 50 km, 100 km and 150 km transmission

of amplification stages on either side of a 0.4 nm tunable band pass filter (TBPF) centered on the test-channel with a VOA for power adjustment. The E-band and S/C/L band signals were separated in a WDM coupler at the receiver input. For S/C/L band signals, a single coherent receiver (CoRx) detected the signal using a 10 kHz linewidth local oscillator (LO). A single tunable filter operating between 1450 nm and 1650 nm was used for all channels with WDM couplers used split and combine signals between per band amplification stages. E-band signals were received with a distinct CoRx with an E-band optimised hybrid, dual-window photodiodes and 200 kHz linewidth LO laser. The signals were acquired by an 80 GS/s real-time oscilloscope that stored traces for offline processing. The throughput of each wavelength channel was estimated from the GMI and independently assessed using LDPC codes from the DVB-S2 standard. Code-rate puncturing was implemented to achieve a bit error rate (BER) below 5×10^{-5} with a 1% overhead outer hard-decision code [27], assumed to remove any remaining bit errors. Signal quality and throughput measurements for each wavelength channel were performed on three 10 µs traces

The transmission fiber was optimised for wideband operation with suppressed OH absorption and loss of 0.24 dB/km, 0.19 dB/km and 0.21 dB/km at 1440 nm, 1560 nm and 1625 nm respectively. For all measurements, the input transmission spectrum was conditioned by the optical processors to have roughly equal power per channel of -4 dBm at the fiber input. For single span measurements, using the scheme shown in Fig. 4(c), over 50 km, 100 km or 150 km spans of SMF, backward propagating Raman pumps were added in a WDM coupler with four 10 nm spaced pumps from 1320 nm to 1350 nm with 250 mW power and a 350 mW 1385 nm pump. A simplex power optimisation was performed by measuring the OSNR of selected channels across the total signal bandwidth. Generally, the highest available pump power for the utlilized wavelengths was found to be optimum, but it was observed that use of available lower wavelength pumps particularly impacted E-band channels and slightly reduced the overall OSNR. For 50 and 100 km transmission, PDM-256QAM was used for S/C/L band signals and PDM-64-QAM for E-band, primarily due to the higher linewidth Tx and LO lasers. For 150 km transmission, PDM-64QAM and PDM-16QAM were used for the S/C/L and E bands, respectively.

For the 200 km amplified span measurement shown in Fig. 4(d), the same Raman pump combination described previously was used with the exception that the 1385 nm pump was removed from the first fiber span after observing a deleterious gain tilt at the beginning of the second span after DFAs. For 200 km transmission PDM-64-QAM modulations was used for all 1050 x 25 GHz spaced, 24.5 GBd transmitted WDM channels. In contrast to the single span measurements, a super luminescent laser diode (SLD), was used as the ASE seed for 200 km measurements, replacing a BDFA with no input signal which was then used in the amplified link.

IV. Results and Discussion

A. Single span transmission

The characteristics of the Raman amplified single fiber span are shown in Fig. 5 (a) for 100 km length. The launched E/S/C/L-band

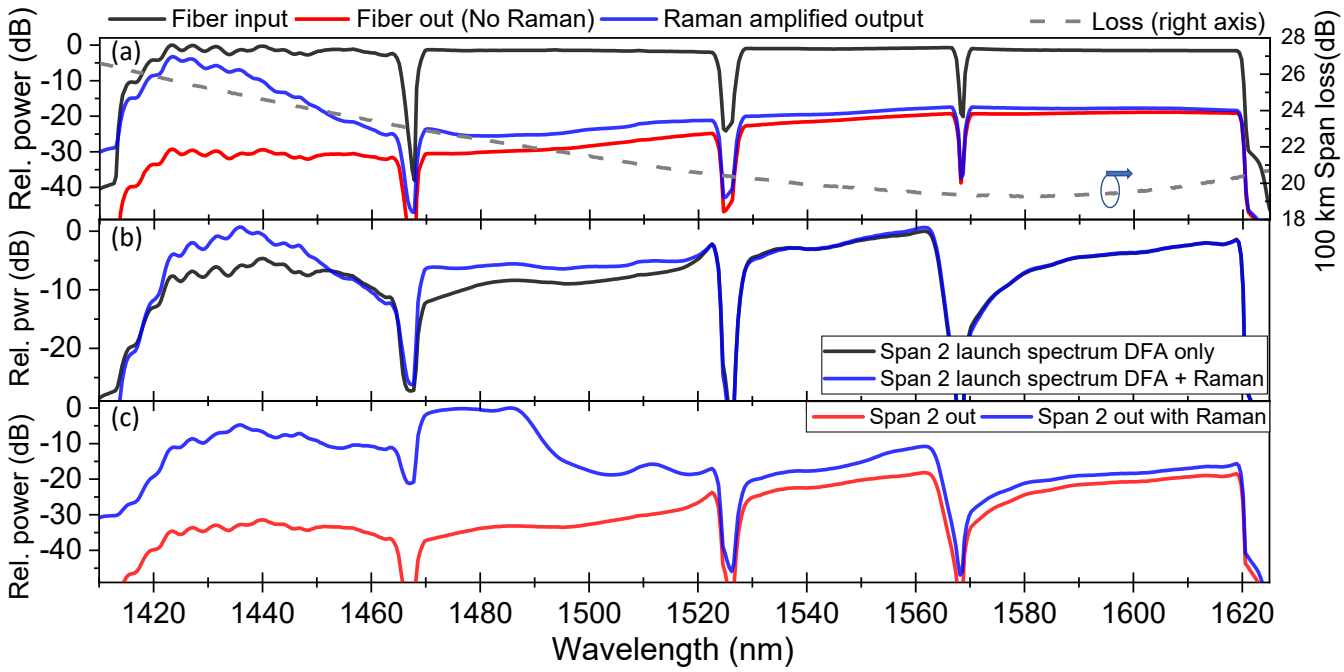

Fig. 6: Wideband signal spectra (a) left-axis E/S/C/L-band signal at input (black) + output (red) of first fiber span with Raman amplification profile (blue). Right-axis span loss of 100 km fiber span, (b) Launch spectra after DFA amplification between spans with and without Raman pumps acting on first span, and (c) output of span 2 with and without Raman amplification in both spans.

input signal (black), becomes tilted at the fiber output before Raman amplification (red) by the combination of stimulated right-axis). The addition of the Raman pumps provides strong gain across the E-band and large parts of the S-band with SRS from those signal channels also boosting C/L-band signals, as shown in the fiber output with Raman, shown in blue. The highest gain is observed for low S-band wavelengths where the ON-OFF Raman gain is similar to the 100 km fiber loss of around 22 dB. Raman scattering (SRS) and the fiber loss profile (Dashed grey,

Figure 5(b) is a summary of signal quality measurements with the highest overall data-rate after 50 km transmission, showing the GMI and decoded data-rates vs. wavelength. The figure shows that high Raman gain and low fiber loss lead to the highest data-rates in S-band and C-band with L-band suffering from low Raman gain and higher EDFA noise figure. E-band data-rates appear affected by the high fiber loss and may in part also be impaired by the impact of higher linewidth from the transmitter and LO lasers used. Lower data-rates are observed at the edges of the DFA gain profiles and the slight slope from low to high wavelengths across E and S-bands is believed to arise from a combination of the wavelength-dependent fiber loss and SRS power transfer that occurs from the start of the link despite the large ON-OFF Raman gain. The combined data-rate of all 1097 WDM channels after 50 km was 321 Tb/s when estimated from the GMI and 301 Tb/s after LDPC decoding, showing the potential improvement possible with optimized coding.

Figure 5(c) shows the GMI estimated data-rate as a function of wavelength after 50 km, 100 km and 150 km transmission. Evident is the increasing impact of the fiber attenuation profile on E and S band channels as the distance increases on top of power transfer resulting from SRS. After 100 km, aside from the lower E-band channels and S-band channels that seem to be affected by the Raman gain profile (Fig. 5(a)), the data-rates are similar to 50 km transmission with a total data-rate reaching 285 Tb/s after decoding and 301 Tb/s based on GMI. After 150 km the GMI and decoded data-rates reduce to 217 Tb/s (decoded) and 239 Tb/s (GMI) with large reductions in per-channel data-rate most evident in E and S-bands. In addition to the growing impact of increasing fiber loss and SRS, the impact of the uneven Raman gain, shown in Fig. 5(a), appears to cause some variation in signal quality across the E-band after 150 km.

B. Amplified two-span 200 km transmission

Figure 6 shows optical spectra at points along the 200 km transmission link. As evident from Fig. 5(c), 150 km spans lead to significant reduction in signal quality in all bands, but the throughput for 100 km transmission is only 6% lower than the 50 km case. Hence, to maximize the transmission distance with a limited number of amplifiers, 100 km fiber spans were selected for multi-span transmission. The characteristics of the first Raman amplified span are shown in Fig. 6 (a). The launched E/S/C/L-band input signal (black) becomes tilted at the fiber output (red) by the combination of stimulated Raman scattering (SRS) and the fiber loss (dashed grey, right-axis). The addition of the 1320-1350 nm Raman pumps provides more than 20 dB gain for low wavelength E-band channels which reduces to around 6 dB for the higher wavelength S-band channels without the 1385 nm pump. As in the single span measurements, SRS from signal channels also boosts the power of C/L-band signals. Some ripples are evident in the E-band input spectrum and arise from an SLD used to generate the dummy channel spectrum which is imperfectly compensated in the

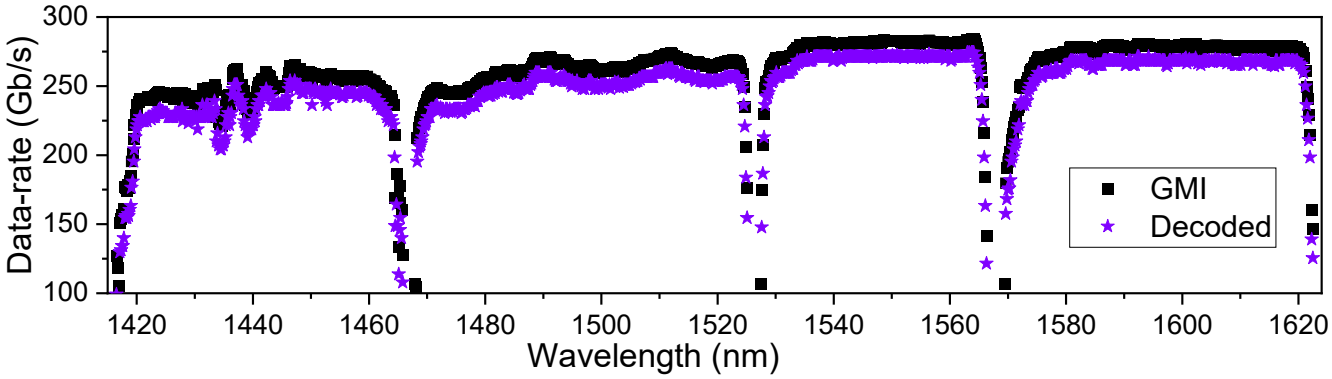

Fig. 7: GMI estimated and LDPC decoded data-rate after 200 km transmission

E-band OP. Fig 6(b) shows the output spectra of the amplification stage after 100 km transmission. The impact of higher input power when utilizing the first span Raman pumps leads to higher output power in the B/T-EDFAs, with little impact on the C/L-band EDFAs. Whilst the C-band profile largely resembles the SRS tilted spectrum at the output of span 1, an additional strong gain tilt is added by the L-band EDFA giving >15 dB power variation across the band. In the 2nd span, the 1385 nm pump that was not used in the 1st span due to bandwidth limiting gain tilt in the BDFA placed after the first 100 km span, provided large gain across E and low S-band channels, as shown in Fig. 6(c), which also again shows that increased SRS boosts the power of C and L-band signals by 3 dB to 10 dB when the Raman pumps are utilized.

The signal quality measurements are summarized in Fig. 7 which shows the GMI-estimated and decoded data-rates as a function of wavelength. The majority of C and L-band channels have a GMI data-rate between 260 Gb/s and 285 Gb/s decreasing at the edge of amplifier gain windows and a small reduction in the L-band region suffering from gain tilt after the 100 km amplification stage. In S-band, the data-rate ranges from 270 Gb/s to around 240 Gb/s at lower wavelengths with some peaks coinciding with gain of Raman pumps evident in Fig.6. In E-band, the per-channel data-rates appear to be conditioned primarily by the Raman amplified spectral shape shown in Fig. 6, with a number of dips in data-rate that are believed to arise from a combination of water absorption in E-band components (OP and TBPF), ripple originating from the SLD that results in variation of channel OSNR after setting test-band power in relation to it, and the Raman amplification spectra. Compared to the results published in [18], the modulator bias stability was improved leading to more consistent E-band signal quality. The combined data-rate of all 1050 WDM channels after 200 km transmission was 270.9 Tb/s when estimated from the GMI and 258.1 Tb/s after LDPC decoding. The per band GMI estimated data-rates were 68.7, 79.8, 54.2 and 68.2 Tb/s from 287, 310, 199 and 254, E, S, C and L-band channels, respectively.

C. Transmission Summary

Table 1. shows a summary of the transmission results reported in the previous parts of section IV. For all distances up to 200 km transmission bandwidths of around 27 THz could be achieved with channels at the edges of the E-band and S band and long wavelength L-band channels being removed at longer distances due to low signal quality. GMI data-rates were around 5-6 % larger than the decoded data-rates, increasing to 10% for lower data-rate signals in the single span 150 km measurements, giving an indication of the highest potential data-rates achievable with better optimized coding. The highest data-rate after 50 km transmission is a 25% increase in the previous highest recorded SMF data-rate but achieved with approximately 35% larger transmission bandwidth showing a reduction in spectral efficiency for E-band signals. We note that E-band transmitter and LO lasers had significantly higher linewidth that may have impacted signal quality of high-order QAM signals compared to SCL band signals that used high-quality stabilized narrow linewidth laser sources.

TABLE I
SUMMARY OF TRANSMISSION DEMONSTRATIONS

Dist. (km)	BW (THz)	No. WDM channels	Data-rate (GMI)	Decoded data-rate
50	27.8	1097	321 Tb/s	301 Tb/s
100	27.2	1076	301 Tb/s	285 Tb/s
150	26.8	1045	239 Tb/s	217 Tb/s
200	27	1050	271 Tb/s	258 Tb/s

The data-rate after 200 km transmission was only around 15% lower than 50 km, showing the potential of longer transmission distances using multiple amplified 100 km spans. The impact of wavelength dependent attenuation and SRS tilt on the signal quality and data-rates, evident in Fig. 6, shows that 150 km spans would lead to quicker degradation of signal quality over multiple spans with the same level of Raman amplification. Overall, these results show that for distances up to 200 km, our newly developed BDFAs and multi-port optical processor support a significant increase in achievable transmission bandwidth and data-rate, adding to the enormous information carrying potential of optical fibers that may also be applicable to previously deployed systems.

V. CONCLUSION

We have constructed an E/S/C/L-band transmission system with over 27 THz of near continuous bandwidth based on a combination of bismuth(B-), thulium(T-), and erbium (E-doped-fiber amplifiers (DFAs) with distributed Raman amplification. The development of BDFA and custom E-band optical processor enabled dense-WDM transmission of high

order QAM signals across the E-band to complement those in S/C and L-bands. After 50 km the full system could receive 1097 x 25 GHz spaced 24.5 GBd PDM-QAM signals from 1410.8 nm to 1623.1 nm. The GMI estimated data-rate of 321 Tb/s or 301 Tb/s after LDPC decoding. This was an increase of 25% on the previous highest data-rate demonstration in standard single-mode fiber. After 2 x 100 km amplified spans, 270.9 Tb/s (258.1 Tb/s decoded) was achieved, showing potential for longer transmission with amplified 100 km spans. Some ripple from water absorption was observed in E-band components and the potential for higher data-rates with optimized E-band components such as modulators and lasers remains. Overall, these results show that E/S/C/L-band transmission enabled by a new BDFA and multi-port OP can increase the information carrying capability of new and deployed optical fiber communication systems.

ACKNOWLEDGMENT

This work is supported by EPSRC Programme Grant ARGON (EP/V000969/1)

REFERENCES

[1] "Cisco Annual Internet Report - Cisco Annual Internet Report (2018–2023) White Paper - Cisco." https://www.cisco.com/c/en/us/solutions/collateral/executive-perspectives/annual-internet-report/white-paper-c11-741490.html (accessed Apr. 13, 2023).

[2] United Nations Conference on Trade and Development, Digital economy report 2019: value creation and capture : implications for developing countries. 2019.

[3] A. Ferrari, A. Napoli, N. Costa, J. K. Fischer, J. Pedro, W. Forysiak, A. Richter, E. Pincemin, and V. Curri, "Multi-Band Optical Systems to Enable Ultra-High Speed Transmissions," in 2019 Conference on Lasers and Electro-Optics Europe and European Quantum Electronics Conference, paper ci_2_3..

[4] J. K. Fischer et al., "Maximizing the Capacity of Installed Optical Fiber Infrastructure Via Wideband Transmission," in 2018 20th International Conference on Transparent Optical Networks (ICTON), Jul. 2018, pp. 1–4. doi: 10.1109/ICTON.2018.8473994.

[5] D. J. Richardson, J. M. Fini, and L. E. Nelson, "Space-division multiplexing in optical fibres," Nat. Photonics, vol. 7, no. 5, pp. 354–362, Apr. 2013, doi: 10.1038/nphoton.2013.94.

[6] B. J. Puttnam, G. Rademacher, and R. S. Luís, "Space-division multiplexing for optical fiber communications," Optica, vol. 8, no. 9, p. 1186, Sep. 2021, doi: 10.1364/OPTICA.427631.

[7] H. Sakr, Y. Hong, T. D. Bradley, G. T. Jasion, J. R. Hayes, H. Kim, I. A. Davidson, E. Numkam Fokoua, Y. Chen, K. R. H. Bottrill, N. Taengnoi, P. Petropoulos, D. J. Richardson, F. Polett, "Hollow Core Optical Fibers for Ultra-Wideband Optical Communications," 2019 Asia Communications and Photonics Conference (ACP), Chengdu, China, 2019

[8] J. Renaudier, A. C. Meseguer, A. Ghazisaeidi, P. Tran, R. R. Muller, R. Brenot, A. Verdier, F. Blache, K. Mekhazni, B. Duval, H. Debregeas, M. Achouche, A. Boutin, F. Morin, L. Letteron, N. Fontaine, Y. Frignac and Gabriel Charlet 'First 100-nm Continuous-Band WDM Transmission System with 115Tb/s Transport over 100km Using Novel Ultra-Wideband Semiconductor Optical Amplifiers', In Proc. European Conference on Optical Communication (ECOC) 2017, paper Th.PDP.A.doi: 10.1109/ECOC.2017.8346084.

[9] J. Renaudier, A. Arnould, D. Le Gac, A. Ghazisaeidi, P. Brindel, M Makhsiyan, A. Verdier, K. Mekhazni, F. Blache, H. Debregeas, A. Boutin, N Fontaine, D Neilson, R. Ryf, H. Chen, M. Achouche and G. Charlet '107 Tb/s Transmission of 103-nm Bandwidth over 3×100 km SSMF using Ultra-Wideband Hybrid Raman/SOA Repeaters', In Proc. Optical Fiber Communication Conference (OFC) 2019, paper Tu3F.2.1

[10] F. Hamaoka et al., "150.3-Tb/s Ultra-Wideband (S, C, and L Bands) Single-Mode Fibre Transmission over 40-km Using >519Gb/s/A PDM-128QAM Signals," in 2018 European Conference on Optical Communication (ECOC),paper Mo4G.1 doi: 10.1109/ECOC.2018.8535140.

[11] B. J. Puttnam, R. S. Luís, G. Rademacher, L. Galdino, D. Lavery, T. A. Eriksson, Y. Awaji, H. Furukawa, P. Bayvel and N. Wada., '0.61 Pb/s S, C, and L-Band Transmission in a 125μm Diameter 4-core Fiber Using a Single Wide-band Comb Source', J. Light. Technol. , vol. 39, no. 4, pp. 1027-1032, 15 Feb.15, 2021, doi: 10.1109/JLT.2020.2990987.

[12] L. Galdino, A. Edwards, W. Yi, E. Sillekens, Y. Wakayama, T. Gerard, W. Sheldon Pelouch, S. Barnes, T. Tsuritani, R. I. Killey, D . Lavery and P. Bayvel 'Optical Fibre Capacity Optimisation via Continuous Bandwidth Amplification and Geometric Shaping', EEE Photonics Technology Letters, vol. 32, no. 17, pp. 1021-1024, 1 Sept.1, 2020, doi: 10.1109/LPT.2020.3007591.

[13] B. J. Puttnam, R. S. Luís, G. Rademacher, M. Mendez-Astudilio, Y. Awaji, and H. Furukawa, "S, C and Extended L-Band Transmission with Doped Fiber and Distributed Raman Amplification," in 2021 Optical Fiber Communications Conference and Exhibition (OFC), paper Fb3.3

[14] B. J. Puttnam, R. S. Luís, G. Rademacher, M. Mendez-Astudillio, Y. Awaji, and H. Furukawa, "S-, C- and L-band transmission over a 157 nm bandwidth using doped fiber and distributed Raman amplification," Opt. Express, vol. 30, no. 6, p. 10011, Mar. 2022, doi: 10.1364/OE.448837.

[15] X. Zhao, S. Escobar-Landero, D. Le Gac, A. Lorences-Riesgo, T. Viret-Denaix, Q. Guo, L. Gan, S. Li, S. Cao, X. Xiao, N. E. Dahdah, A. Gallet, S. Yu, H. Hafermann, L. Godard, R. Brenot, Y. Frignac, and G. Charlet, "2005 Tb/s Transmission with S+C+L Amplification Covering 150 nm Bandwidth over 2×100 km PSCF Spans," in European Conference on Optical Communication (ECOC) 2022, paper Th3C.4.

[16] D. Soma et al., "25-THz O+S+C+L+U-Band Digital Coherent DWDM Transmission Using a Deployed Fibre-Optic Cable" ECOC'23 paper Th.C.2.4.

[17] B. J. Puttnam et al., "301 Tb/s E, S, C+L-Band Transmission over 212 nm bandwidth with E-band Bismuth-Doped Fiber Amplifier and Gain Equalizer" ECOC'23 paper Th.C.2.4.

[18] B. J. Puttnam et al., 264.7 Tb/s E, S, C + L-Band Transmission over 200 km' Submitted to Optical Fiber Conference 2024, result expected December 2023

[19] A. Donodin, P. Hazarika, M. Tan, V. Dvoyrin, M. Patel, I. Phillips, P. Harper, S. Turitsyn, and W. Forysiak, "195-nm Multi-Band Amplifier Enabled by Bismuth-doped Fiber and Discrete Raman Amplification," in European Conference on Optical Communication (ECOC) 2022, paper Th2A.1.

[20] A. Donodin et al., 'Bismuth doped fibre amplifier operating in E- and S-optical bands', Opt. Mater. Express, vol. 11, no. 1, p. 127, Jan. 2021, doi: 10.1364/OME.411466.

[21] Z. Zhai, A. Halder, Jayanta Sahu, "E+S-band Bismuth-doped Fiber Amplifier with 40dB Gain and 1.14dB Gain per Unit Length" Proc. European Conference on Optical Communication (ECOC) 2023 paper Th. C.1.1

[22] P. Hazarika, M. Tan, A. Donodin, I. Phillips, P. Harper, M.J. Li, and W. Forysiak, "210 nm E, S, C and L band multistage discrete Raman amplifier," in Optical Fiber Communication Conference (OFC) 2022. 2022, p. Tu3E.2

[23] Y. Wang, N. K. Thipparapu, D. J. Richardson and J. K. Sahu, "Ultra-Broadband Bismuth-Doped Fiber Amplifier Covering a 115-nm Bandwidth in the O and E Bands," in Journal of Lightwave Technology, vol. 39, no. 3, pp. 795-800, 1 Feb.1, 2021, doi: 10.1109/JLT.2020.3039827.

[24] Y. Ososkov, A. Khegai, S.Firstov, K. Riumkin, S. Alyshev, Alexander Kharakhordin, A. Lobanov, A. Guryanov, and M. Melkumov, "Pump-efficient flattop O+E-bands bismuth-doped fiber amplifier with 116 nm – 3 dB gain bandwidth," Opt. Express 29, 44138-44145 (2021)

[25] N. K. Fontaine, I. D. Phillips, W. Forysiak, L Dallachiesa, M. Mazure, R, Ryf, H, Chen and D, T. Nielson, "Multiport E-band Wavelength equalizer," in 2023 European Conference on Optical Communication (ECOC), paper P86

[26] D.J. Elson, G. Saavedra, K. Shi, D. Semrau, L. Galdino, R. Killey, B. C. Thomsen, and P. Bayvel, "Investigation of bandwidth loading in optical fibre transmission using amplified spontaneous emission noise," Opt. Express 25, 19529-19537 (2017)

[27] D. S. Millar, R. Maher, D. Lavery, T. Koike-Akino, M. Pajovic, A. Alvarado, M. Paskov, K. Kojima, K. Parsons, B. C. Thomsen, S. J.

Savory and P. Bayvel., 'Design of a 1 Tb/s Superchannel Coherent Receiver', J. Light. Technol., vol. 34, no. 6, pp. 1453–1463, Mar. 2016, doi: 10.1109/JLT.2016.2519260.